

1 Methods in Ecology and Evolution

2

3 Standard paper

4

5 Title:

6 **Detecting evolutionarily significant units above the species level using the**

7 **Generalized Mixed Yule Coalescent method**

8

9 Running title: Detecting ESUs above the species

10

11 Word count: 6876

12

13 **Aelys M. Humphreys^{1,2}, Catarina Rydin², Knud A. Jønsson^{1,3}, David Alsop^{1,3}, Leah M.**
14 **Callender-Crowe^{1,3,4} and Timothy G. Barraclough¹**

15

16 ¹*Department of Life Sciences, Imperial College London, Silwood Park Campus, Ascot,*
17 *Berkshire SL5 7PY, UK*

18 ²*Department of Ecology, Environment and Plant Sciences, Stockholm University, 10691*
19 *Stockholm, Sweden*

20 ³*Department of Life Sciences, Natural History Museum, Cromwell Road, London SW7 5BD,*
21 *UK*

22 ⁴*Current address: Faculty of Life Sciences, University of Manchester, Manchester M13 9PT,*
23 *UK*

24

25 Author for correspondence:

26 Aelys Humphreys

27 Department of Ecology, Environment and Plant Sciences

28 Stockholm University

29 SE-106 91 Stockholm, Sweden

30 Email: aelys.humphreys@su.se

31 **Summary**

32 1. There is renewed interest in inferring evolutionary history by modelling diversification
33 rates using phylogenies. Understanding the performance of the methods used under different
34 scenarios is essential for assessing empirical results. Recently we introduced a new approach
35 for analysing broadscale diversity patterns, using the Generalized Mixed Yule Coalescent
36 (GMYC) method to test for the existence of evolutionarily significant units above the species
37 (higher ESUs). This approach focuses on identifying clades as well as estimating rates and we
38 refer to it as clade-dependent. However, the ability of the GMYC to detect the phylogenetic
39 signature of higher ESUs has not been fully explored, nor has it been placed in the context of
40 other, clade-independent approaches.

41 2. We simulated >32,000 trees under two clade-independent models: constant-rate birth-death
42 (CRBD) and variable-rate birth-death (VRBD), using parameter estimates from nine
43 empirical trees and more general parameter values. The simulated trees were used to evaluate
44 scenarios under which GMYC might incorrectly detect the presence of higher ESUs.

45 3. The GMYC null model was rejected at a high rate on CRBD-simulated trees. This would
46 lead to spurious inference of higher ESUs. However, the support for the GMYC model was
47 significantly greater in most of the empirical clades than expected under a CRBD process.
48 Simulations with empirically derived parameter values could therefore be used to exclude
49 CRBD as an explanation for diversification patterns. In contrast, a VRBD process could not
50 be ruled out as an alternative explanation for the apparent signature of hESUs in the empirical
51 clades, based on the GMYC method alone. Other metrics of tree shape, however, differed
52 notably between the empirical and VRBD-simulated trees. These metrics could be used in
53 future to distinguish clade-dependent and clade-independent models.

54 4. In conclusion, detection of higher ESUs using the GMYC is robust against some clade-
55 independent models, as long as simulations are used to evaluate these alternatives, but not
56 against others. The differences between clade-dependent and clade-independent processes are
57 biologically interesting, but most current models focus on the latter. We advocate more
58 research into clade-dependent models for broad diversity patterns.

59

60 **Keywords:** birth-death, clade-dependent, clade-independent, diversification, phylogenetic
61 clustering, rate shift, relative extinction rate, simulation

62

63 **Introduction**

64 There is currently widespread interest in understanding the evolutionary history of clades by
65 inferring diversification dynamics from phylogenetic trees. Of particular interest has been
66 identifying shifts in net diversification rates (Rabosky 2006; Alfaro *et al.* 2009) or rapidly
67 diversifying clades (e.g. Hughes & Eastwood 2006; Valente, Savolainen & Vargas 2010) that
68 might be associated with a particular trait or region (Maddison, Midford & Otto 2007;
69 Goldberg, Lancaster & Ree 2011). Recent advances have focussed on making the widely used
70 birth-death model (Nee, May & Harvey 1994) more flexible, allowing rates to vary more
71 generally over time (Morlon, Parsons & Plotkin 2011), as a function of standing diversity
72 (Etienne *et al.* 2012) or among lineages, to identify clades undergoing adaptive radiation
73 (Etienne & Haegeman 2012) or with shared evolutionary dynamics (Rabosky 2014).

74 What processes could cause sharing and decoupling of rates among lineages?
75 Recently, we proposed a model of evolutionarily significant units above the level of species
76 (Barraclough 2010; Humphreys & Barraclough 2014). This model assumes that i) species
77 within a wider clade occupy a range of geographical regions and/or ecological zones; ii) there
78 are separate limits on the number of species within each geographical region or ecological
79 zone; iii) species turnover occurs through ongoing speciation and extinction and iv)
80 transitions between geographical regions or ecological zones are rare, meaning that closely
81 related species tend to occupy the same region and/or zone. If these conditions are met, then
82 species will fall into a set of clades, each of which occupies a separate geographical region or
83 ecological zone, which we call higher evolutionarily significant units (hESUs; Fig. 1).
84 Because of ongoing species turnover, species within a hESU share evolutionary fate as well
85 as history (Barraclough & Humphreys 2015). This means that any event influencing the
86 likelihood of lineages speciating or going extinct will be shared among species within but not
87 among hESUs; hence, diversification rates are shared within and decoupled among hESUs.

88 The hESU model thus provides an explanation for diversity patterns that focuses on
89 identifying units (clades) as well as estimating diversification rates. We therefore refer to it as
90 a clade-dependent model (Fig. 1). The phylogenetic signature of hESUs is a significant
91 increase in the rate of lineage accumulation toward the present. However, such a pattern may
92 equally result from a clade-wide increase in diversification rates caused, for example, by a
93 rebound from a mass extinction event (Crisp & Cook 2009) or a burst following
94 environmental change (Stadler 2011). In other words, the pattern of an increase in branching
95 rate, predicted to arise with hESUs, could also result from a uniform change in diversification
96 rate, acting across an entire clade or independently of clade membership (clade-independent
97 model, Fig. 1). Indeed, distinguishing alternative models for diversification is challenging

98 because several processes can lead to indistinguishable patterns (Barracough & Nee 2001;
99 Rabosky 2009; Morlon, Potts & Plotkin 2010; Moen & Morlon 2014). Understanding the
100 performance of the models used to study these patterns is therefore necessary if we are to
101 have confidence in empirical inferences.

102 Here we use simulations to explore error rates of the generalised mixed Yule
103 coalescent (GMYC; Pons *et al.* 2006) method, used to define hESUs, when trees actually
104 derive from clade-independent processes. The GMYC method analyses waiting times
105 between branching events in a time-calibrated phylogeny, where tips represent species,
106 densely sampled (Humphreys & Barracough 2014) for a broader clade, to identify significant
107 shift(s) in the rate of branching. The approach uses a null model that no shift has occurred and
108 that a single process is sufficient to describe phylogenetic branching across the entire clade.
109 The alternative model finds one (single threshold version, ST) or more (multiple threshold
110 version, MT) shifts in branching rate toward the present (Pons *et al.* 2006; Fontaneto *et al.*
111 2007; Monaghan *et al.* 2009; Fujisawa & Barracough 2013), denoting the transition from
112 among to within hESU branching. In its current formulation, the alternative model thus uses
113 two branching parameters, λ , to explain the distribution of waiting times, one within and one
114 among hESUs. In addition, the GMYC algorithm includes one (null) or two (ST, MT) scaling
115 parameters, p , that allow the net branching rate to depart from a constant-rate process ($p = 1$),
116 to either accelerate ($p > 1$) or decelerate ($p < 1$) toward the present.

117 Several studies have assessed the factors that influence the performance of the GMYC
118 method applied at the species level (e.g. Papadopoulou *et al.* 2008; Reid & Carstens 2012;
119 Fujisawa & Barracough 2013; Tang *et al.* 2014), the main factor being the level of variation
120 within species relative to divergence times among species (Fujisawa & Barracough 2013).
121 For analyses of higher clades, we previously recorded high error rates for trees simulated
122 under a particular clade-independent model (with constant extinction rates), but found that
123 empirical signatures of hESUs in were significantly stronger than expected under that model
124 (Humphreys & Barracough 2014). We build on these results here to assess error rates for a
125 broader range of clade sizes, extinction rates and diversification processes. We examine
126 performance of the GMYC approach on empirical trees and trees simulated under two
127 different clade-independent processes that might generate similar phylogenetic patterns to the
128 hESU model: constant-rate birth-death (CRBD) and variable-rate birth-death (VRBD) with a
129 tree-wide shift in diversification rate. The CRBD model, commonly used for
130 macroevolutionary analyses, generates an upturn in apparent branching rate towards the
131 present when extinction rates are high (Nee *et al.* 1994). This might artefactually lead to the
132 detection of hESUs using the standard GMYC method. Simulated trees were therefore used to

133 estimate the rate of incorrect detection of hESUs for data generated using a CRBD model.
134 More challenging still, the VRBD model generates a simultaneous increase in branching rate
135 across an entire clade. This pattern should be indistinguishable from the predictions of hESUs
136 as detected using the ST version of GMYC. There is no reason, however, to expect
137 simultaneous transition times for all hESUs in a clade-dependent model and therefore the MT
138 version of the GMYC might still reveal stronger evidence for hESUs than a VRBD model.

139 To focus our investigation on real datasets, we ran the simulations using parameter
140 values estimated for nine empirical clades. We then compared the significance of hESUs in
141 each clade relative to the standard GMYC null model, to trees simulated assuming a CRBD
142 model, and to trees simulated assuming a VRBD model. Empirical trees yielded higher
143 likelihoods under the alternative GMYC model than did trees simulated under the CRBD
144 model, indicating that inferences of hESUs are robust to the effects of constant extinction
145 rates on tree shapes. The likelihoods of empirical trees under the GMYC model were not,
146 however, higher than expected under the VRBD model, even using the MT version.
147 Additional measures of tree shape or of ecological trait variation are necessary to distinguish a
148 signal of clade-dependent hESUs from a VRBD model.

149

150 **Materials and methods**

151

152 PHYLOGENETIC TREES FOR EMPIRICAL DATA

153 Empirical analyses were performed for nine clades, defined as representing at least one order
154 and a manageable number of species (≤ 1000 species), for which densely sampled, time
155 calibrated phylogenies were available or could be generated using published data. Such
156 phylogenies were available for three clades of mammals (Carnivora, Euungulata and
157 Lagomorpha; Humphreys & Barraclough 2014), birds (Afroaves (sensu Jarvis *et al.* 2014),
158 nightbirds (except owls), swifts and hummingbirds (sensu Ericson *et al.* 2006, hereafter
159 'nightbirds') and core waterbirds plus pigeons and cuckoos (hereafter 'waterbirds'; Jetz *et al.*
160 2012; SI Text)) and conifers (Leslie *et al.* 2012). Phylogenies for cycads and Gnetales were
161 generated using standard protocols from published matK, rbcL, 18S and, for cycads, PHYP
162 sequences (Rydin & Korall 2009; Nagalingum *et al.* 2011; Hou *et al.* 2015; SI Text). Overall,
163 all orders, families and genera in these clades were sampled and on average 80-90% of the
164 species (Table S2).

165

166 GENERALISED MIXED YULE-COALESCENT ANALYSES FOR EMPIRICAL TREES

167 Null, ST and MT GMYC models were fitted to each bird and gymnosperm maximum clade

168 credibility (MCC) tree using the R (R Development Core Team 2011) package splits (Ezard,
169 Fujisawa & Barraclough 2014). The null model has two parameters (λ , p) and the alternative
170 models four (λ_{among} , p_{among} , λ_{within} , p_{within}). The inferred threshold time does not constitute a
171 model parameter but a constraint to model search space (Fujisawa & Barraclough 2013).
172 Model inferences were summarised across the 95% confidence set of models. Mammal results
173 were obtained from Humphreys & Barraclough (2014).

174

175 SIMULATING BIRTH-DEATH TREES WITH EMPIRICAL PARAMETER VALUES

176 To study the behaviour of GMYC models under alternative scenarios, CRBD trees (Nee, May
177 & Harvey 1994) with the properties of each of the nine empirical clades (number of tips,
178 speciation (λ) and extinction (μ) rates) were simulated. Parameter values were estimated using
179 the birthdeath function in the R package ape (Paradis, Claude & Strimmer 2004), applied to
180 500 trees for all datasets except conifers, where a single tree was used. Five hundred CRBD
181 trees were simulated using λ and relative extinction ($\mu/\lambda = \epsilon$) rates sampled randomly from
182 across the range of estimates for each clade using sim.bd.taxa in TreeSim (Stadler 2012) and
183 drop.extinct in Geiger (Harmon *et al.* 2008). The estimate of ϵ for Gnetales was always 1.00
184 (Table S3) so trees were simulated with this parameter sampled between 0.98-0.99 to speed
185 up the simulations. For the conifer CRBD trees, parameters were sampled from the same
186 range as for cycads because the point estimate for conifers was identical to the median
187 estimate for cycads. This resulted in 9 x 500 CRBD trees of varying size, λ and ϵ (Table S3).
188 Finally, null, ST and MT GMYC models were fitted to each simulated tree and the difference
189 in fit between null and alternative models determined using likelihood ratio (LR) tests. Error
190 rates for CRBD trees were recorded as the proportion of trees in each set for which the null
191 model was rejected. Note these are not type I error rates, but errors due to the null model
192 being rejected in favour of the GMYC model when in fact a third model is true (i.e. CRBD).

193

194 SIMULATING BIRTH-DEATH TREES WITH GENERAL PARAMETER VALUES

195 To test GMYC performance above the species more generally, trees were simulated under a
196 pure birth model ($\epsilon=0$; Yule 1925) and CRBD models with $\epsilon = 0.1, 0.3, 0.5, 0.7$ and 0.9 . Pure
197 birth trees were simulated using the tree.bd function in diversitree (FitzJohn 2012), “low” ϵ
198 trees ($\epsilon = 0.1, 0.3$) using sim.bdtree in Geiger and “high” ϵ trees ($\epsilon = 0.5, 0.7, 0.9$) using
199 sim.bd.taxa in TreeSim and drop.extinct in Geiger. The speciation rate was set to 1.0 for all
200 simulations. For each rate of ϵ 500 trees were simulated, each with 100, 500 and 1000 tips.
201 From these, sets of trees with 100%, 75% and 50% sampling were generated. Removing tips
202 changes the shape of the lineages-through-time (LTT) plot, generating trees with an excess of

203 early branching events (“slowdown”) or, under high rates of ϵ , a less severe “pull of the
204 present” effect. The sets of pruned trees therefore allowed assessing GMYC performance
205 under departures from CRBD. In all, this resulted in 9 x 500 trees for each level of ϵ , i.e., a
206 total of 54 x 500 CRBD trees of varying size, ϵ and branching process. Null, ST and MT
207 GMYC models were fitted to each tree in turn and error rates recorded as above.

208

209 SIMULATING BIRTH-DEATH TREES WITH A CLADE-WIDE SHIFT IN RATES

210 To generate the phylogenetic signature of a clade-wide shift in rates and test the performance
211 of the GMYC method under this scenario, VRBD trees were simulated using the empirically
212 estimated shift position (T , threshold time in absolute time) and ratio of within:among hESU
213 branching rate ($\lambda_{\text{within}}:\lambda_{\text{among}}$, interpreted as pre-shift and post-shift diversification rates,
214 respectively, starting at the present and going back in time), scaled to match rates expected
215 under a CRBD process (SI Text). Trees were simulated using `sim.rateshift.taxa` in TreeSim
216 and nine combinations of parameters and tree characteristics obtained from the empirical
217 clades (Table S4). Parameters were: λ_{among} , λ_{within} and ϵ , randomly sampled from the estimates
218 across 500 trees. Tree characteristics (constraints to reconstructed tree space; Stadler 2011)
219 were: clade size (number of extant tips) and location of the rate shift, expressed in absolute
220 time and sampled randomly from the range of mean threshold times retained among the
221 confidence set of GMYC models for each dataset. This resulted in 9 x 100 VRBD trees of
222 varying size, overall λ , ϵ and position and severity of the rate shift. Null, ST and MT GMYC
223 models were fitted to each tree in turn as above and the proportion of trees for which 1) the
224 null was rejected in favour of the ST-GMYC, 2) the correct empirical position of the rate shift
225 was recovered and 3) fit of the MT-GMYC was significantly better than ST-GMYC ($\Delta\text{AIC} \geq$
226 5; a somewhat conservative cutoff (Burnham & Anderson 2002), due to known sensitivity of
227 MT-GMYC (Fujisawa & Barraclough 2013)) was recorded.

228

229 TREE CHARACTERISTICS

230 Clade size, root age, ϵ , clade imbalance and tree stemminess were recorded for each empirical
231 and simulated tree to assess to what extent the simulated process captured other features of
232 the empirical trees and what affects performance of the GMYC method. Tree imbalance was
233 estimated using Colless’ (I_c ; Colless 1982; Heard 1992) and Sackin’s (I_s ; Shao & Sokal
234 1990) indices because they have been found to perform well compared to other measures
235 (Agapow & Purvis 2002). The former uses the difference in the number of nodes arising from
236 the sister clades of each node and the latter the number of nodes that separates each tip from
237 the root. In general, more imbalanced trees have a higher value under both indexes. To enable

238 comparison among datasets they were normalized using a Yule model (Blum, François &
239 Janson 2006). Tree stemminess was estimated using the non-cumulative stemminess index
240 (St_N ; Rohlf *et al.* 1990). Stemmier trees, i.e. those that have longer unbranched edges, have a
241 higher value. However, values also tend to increase with increasing clade size so St_N was only
242 compared among trees within each size set. Each index was calculated using apTreeshape (Ic
243 and Is; Bortolussi *et al.* 2012) and customized R scripts (St_N ; SI Text). Tree characteristics
244 were correlated against error rates using linear regressions and Generalised Additive Models
245 (Hastie & Tibshirani 1990) using the R package mgcv (Wood 2000; Wood 2011).

246

247 **Results**

248

249 GENERALISED MIXED YULE-COALESCENT RESULTS FOR EMPIRICAL CLADES

250 The GMYC null model was rejected in favour of the ST model for all clades except
251 waterbirds and in favour of the MT model for all clades (Table 1). Only MT models were
252 retained in the 95% confidence set of models for euungulates, conifers, Afroaves and
253 nightbirds, both ST and MT models were retained for carnivores, lagomorphs, cycads and
254 Gnetales and for waterbirds the null was included as well. Based on the confidence set of
255 models, hESUs date to the Miocene (mean threshold: 5.65 Ma [Gnetales] – 16.4 Ma
256 [conifers]; Table 1, Fig. S1) and correspond to traditionally named genera (gymnosperms,
257 mammals), families (mammals) or clades of subfamilial, generic or subgeneric rank (birds;
258 Fig. S2).

259

260 CONSTANT-RATE BIRTH-DEATH SIMULATED TREES

261 As suspected, the standard GMYC method often erroneously detected hESUs from CRBD
262 trees. Error rates for CRBD trees based on empirical parameter estimates ranged from 6.6%–
263 56.8% for ST and 21.1%–88.9% for MT GMYC, being lowest in trees simulated using
264 carnivore parameter values and highest in those based on conifers (Table 2). There is no effect
265 of clade size on error rates (linear regression ST: $F = 0.28$ on 7 d.f., $P = 0.61$; MT: $F = 0.02$ on
266 7 d.f., $P = 0.89$) but error rates increase with increasing ϵ (linear regression ST: $F = 24.4$ on 7
267 d.f., $P = 0.0017$, $R^2 = 0.78$; MT: $F = 29.1$ on 7 d.f., $P = 0.0010$, $R^2 = 0.81$). There is no
268 interaction between clade size and ϵ and the relationship is stronger for MT than ST GMYC
269 (slope = 49 and 26, respectively; Fig. 2).

270 Results for CRBD trees simulated with general parameters confirm these results (Fig.
271 2). Error rates increased non-linearly for all datasets except MT-GMYC with 100% sampling.
272 For the other sets of trees, error rates remained around 10% (ST) and 30% (MT) until $\epsilon = 0.3$,

273 when they increased, non-linearly. The best regression model is a Gaussian process, which is
274 indistinguishable from a quadratic polynomial model, based on AIC values (Table S5).
275 Overall, error rates were higher for MT-GMYC and for higher levels of sampling. This is not
276 because clades with more complete sampling are larger but because they have LTT plots with
277 a more pronounced upturn (Fig. S3; the effect of sampling was marginally significant for the
278 MT results when all clades were analysed together, $P = 0.047$).

279 Despite these effects, the empirical results are generally not explained by incorrect
280 rejection of the null model due to constant-rate birth-death processes: the LR difference in fit
281 between null and alternative GMYC models is much greater for empirical trees than CRBD-
282 simulated trees for both ST and MT models and for all clades except Gnetales and waterbirds
283 (Table 2). Thus, the evidence for hESUs is robust with respect to an alternative CRBD model.

284

285 VARIABLE-RATE BIRTH-DEATH SIMULATED TREES

286 The ST-GMYC detected a shift in $\geq 94\%$ of trees for all datasets except those based on
287 carnivore (47%) and lagomorph (75%) parameter values (Table 3). The simulated position of
288 the shift was correctly inferred on average (estimated threshold time overlaps with range of
289 threshold times under which trees were simulated) for all clades except those based on
290 Afroaves values (Fig. S4). Fit of MT-GMYC was indistinguishable from ST-GMYC for the
291 cycad-based trees and possibly those simulated using Gnetales parameter values (94% and
292 90% of simulated trees, respectively) but significantly better for all other datasets (in 14%–
293 67% of simulated trees; Table S6).

294 The likelihood of the GMYC model for the empirical trees, however, was not greater
295 than expected from VRBD-simulated trees, for either ST or MT versions. Indeed, for both
296 versions, the empirical LR between null and alternative GMYC models was lower for the
297 empirical trees than for the simulated VRBD trees (Table 4).

298

299 CHARACTERISTICS OF SIMULATED VERSUS EMPIRICAL TREES

300 The root height of the CRBD trees encompassed the root height of the empirical trees for all
301 datasets except those based on euungulate and lagomorph parameter estimates, where
302 simulated trees were too young (Fig. S1). The shape of the CRBD trees differed from the
303 empirical trees by having too few deep lineages (carnivores, euungulates, conifers and all
304 three bird clades), a less severe upturn in branching rate (lagomorphs, cycads and Gnetales)
305 and by being more balanced and/or stemmy (Table S7). Exceptions are simulated trees based
306 on carnivore, lagomorph and cycad parameter values, which were indistinguishable from
307 empirical trees for both balance and stemminess.

308 The root height for VRBD trees was extremely old for all simulated trees, except those
309 based on carnivore (overlapped empirical trees) and Afroaves (younger than empirical trees)
310 parameter estimates (Fig. S4). The shape of the VRBD trees approximated that of the
311 empirical tree for carnivore-based trees but differed in various ways for the other datasets. For
312 example, VRBD conifer-based trees had too few surviving old lineages compared to the
313 empirical tree, a completely different shape for all three simulated sets based on bird
314 parameter values and were generally more balanced and/or stemmy than empirical trees
315 (Table S7). Exceptions are trees based on carnivore and lagomorph parameter values, which
316 were indistinguishable from empirical trees for both balance and stemminess.

317

318 **Discussion**

319

320 Our results show that the standard GMYC method is sensitive to high rates of extinction
321 (above approximately 30% of the speciation rate) in CRBD models. Although the scaling
322 parameters, p , were developed to allow for departures from a pure birth model, a constant
323 extinction rate produces a recent upturn in branching rates rather than a gradual increase
324 through the whole tree (Nee *et al.* 1994). This problem becomes more severe with increasing
325 extinction rates but is relatively unaffected by clade size and ameliorated by incomplete
326 sampling (c.f. Fujisawa & Barraclough 2013).

327 One solution, however, is to use a critical value for significance obtained from
328 simulations (e.g. Maddison, Midford & Otto 2007; FitzJohn, Maddison & Otto 2009;
329 Humphreys & Barraclough 2014). This entails comparing the LR difference in fit between
330 null and alternative models for simulated data to that estimated from the empirical data. Using
331 our CRBD simulations for this purpose reveals that the difference in fit between null and
332 alternative models is significantly greater for empirical than simulated trees for all clades
333 except Gnetales and waterbirds ($P < 0.01$; for lagomorphs, $P = 0.05$). For the other seven
334 clades the CRBD model can be excluded. We therefore recommend use of simulations with
335 empirical parameter values to judge significance of the GMYC model against alternative,
336 clade-independent models. Based on the clades analysed here, a general rule of thumb seems
337 to be that a $LR \geq 15$ (ST) and ≥ 20 (MT) compared to the null model is indicative of empirical
338 results that differ significantly from those expected under a BD process at $P = 0.05$ (Table 2).
339 It is also possible to use specific estimates of the LR difference needed for significance for a
340 given extinction rate, ϵ (Fig. 3).

341 In contrast, and as expected, the GMYC model could not discriminate clade-
342 dependent hESUs from a clade-independent VRBD model, where the whole clade

343 experienced a single shift in diversification rate (e.g. due to a change in environmental
344 conditions). In some circumstances the GMYC model might still be able to distinguish these
345 scenarios: for example, if origination of hESUs is staggered in time so that the most recent
346 among-unit branching event postdates the most ancient within-unit branching event
347 (Monaghan *et al.* 2009; Fujisawa & Barraclough 2013), but not in the clades analysed here.

348 How might we refine comparison of these alternatives, which are biologically
349 interesting? The GMYC approach focuses on waiting intervals between branching events, but
350 other features of tree shape might discriminate clade-dependent and clade-independent
351 models. One possibility for improving model discrimination in future is to include additional
352 metrics in model evaluation. We found that the clade-independent models analysed here do a
353 poor job at capturing features of real (empirical) phylogenies. For example, the root height of
354 VRBD trees is generally ridiculously old, e.g. on average 13.7 *billion* years for cycads, ~900
355 Ma for conifers and Gnetales and ~500 Ma for lagomorphs. In addition, there is a tendency
356 for both CRBD and VRBD trees to be more balanced and stemmy than empirical trees but
357 VRBD trees differ more from the empirical trees than do the CRBD trees, despite being
358 simulated to more closely capture the LTT pattern of the empirical trees. The finding that
359 CRBD models do not capture the shape of empirical trees is not new (Mooers & Heard 1997;
360 Nee 2006) but less is known about VRBD models in this respect. Beyond this, and rather than
361 comparing just one null and alternative model, a broad array of models could in principle be
362 fitted to identify a confidence set of plausible models and parameter estimates consistent with
363 the data.

364 Other considerations argue for biological relevance of the detected hESUs, whether
365 those units result from a clade-dependent or clade-independent VRBD process. The hESUs
366 correspond to various taxonomic ranks, revealing taxonomic inconsistencies among groups
367 that are not surprising (e.g. Avise & Johns 1999; Holt & Jönsson 2014). However, the
368 correspondence of hESUs with traditionally named taxa is striking for both mammals
369 (families and genera) and gymnosperms (genera), suggesting that future efforts to understand
370 diversification dynamics in these groups should focus on these ranks. There is less
371 correspondence of bird hESUs with named higher taxa, although these results might be
372 premature because the phylogenies analysed here are based on data for two thirds of the
373 species only (Jetz *et al.* 2012). Intriguingly, the average age of hESUs in each bird, mammal
374 and gymnosperm clade dates to the Miocene. In theory, this does not necessarily mean that
375 anything special happened at that time (Fig. 1, and see Barraclough & Humphreys 2015) but
376 might suggest similar, average turnover rates across clades. Previous analyses of birds and
377 conifers have identified high rates of species turnover in regions characterised by climate

378 fluctuations during the Neogene, including high latitude regions of the Northern Hemisphere
379 and mountainous regions (Jetz *et al.* 2012; Leslie *et al.* 2012). Our results suggest not only
380 general rules governing turnover rates among regions but that different types of organisms
381 occupying these regions might be similarly affected by these rate-governing processes.
382 Further research is needed to determine the causality and generality of these findings.

383 In conclusion, we have shown how inferences of hESU using the GMYC method are
384 robust against some clade-independent models (CRBD), as long as simulations are used to
385 evaluate these alternatives, but not against others (VRBD) that generate very similar patterns
386 in waiting intervals between branching events. The differences between clade-dependent and
387 clade-independent models are interesting biologically, however, and additional metrics either
388 of tree-shape or evaluation of ecological trait distributions (Humphreys & Barraclough 2014)
389 are needed to discriminate these alternatives. We suspect that clade-dependent models,
390 focussing both on diversification rates and the units within which they operate, will prove
391 important for explaining broadscale diversity patterns and encourage more research on this
392 class of models.

393

394 **Acknowledgements**

395 Thanks to Daniele Silvestro for providing a ‘time.limit’ script and Andrew Leslie for the
396 conifer tree. AMH acknowledges the Swedish Research Council Formas (grant 2012-1022-
397 215) and Carl Tryggers Stiftelse (grant CTS-12:409) for funding. CR acknowledges the
398 Swedish Research Council (grant 2010-5497). KAJ acknowledges support from the People
399 Programme (Marie Curie Actions) of the European Union's Seventh Framework Programme
400 (FP7/2007-2013) under REA grant agreement no. PIEF-GA-2011-300924. Analyses were
401 performed using the Imperial College High Performance Computing Service
402 ([http://www.imperial.ac.uk/ict/services/teachingandresearchservices/highperformancecomputi](http://www.imperial.ac.uk/ict/services/teachingandresearchservices/highperformancecomputing)
403 [ng](http://www.imperial.ac.uk/ict/services/teachingandresearchservices/highperformancecomputing)). We thank Emmanuel Paradis and three anonymous reviewers for comments that
404 improved earlier drafts.

405

406 **Data Accessibility**

407 The R code used to calculate the non-cumulative stemminess index (S_{t_N}) is provided as online
408 supporting information (SI Text S4). Trees simulated using empirical parameter values have
409 been deposited in the Dryad Data Repository (doi: 10.5061/dryad.3rt26), as have the Gnetales
410 and cycad trees. Mammal trees can be found in TreeBASE (study ID S15307).

411

412 **References**

- 413 Agapow, P.-M. & Purvis, A. (2002) Power of eight tree shape statistics to detect nonrandom
414 diversification: A comparison by simulation of two models of cladogenesis.
415 *Systematic Biology*, **51**, 866-872.
- 416 Alfaro, M.E., Santini, F., Brock, C., Alamillo, H., Dornburg, A., Rabosky, D.L., Carnevale,
417 G. & Harmon, L.J. (2009) Nine exceptional radiations plus high turnover explain
418 species diversity in jawed vertebrates. *Proceedings of the National Academy of*
419 *Sciences*, **106**, 13410-13414.
- 420 Avise, J.C. & Johns, G.C. (1999) Proposal for a standardised temporal scheme of biological
421 classification for extant species. *Proceedings of the National Academy of Sciences*, **96**,
422 7358-7363.
- 423 Barraclough, T.G. (2010) Evolving entities: towards a unified framework for understanding
424 diversity at the species and higher levels. *Philosophical Transactions of the Royal*
425 *Society B-Biological Sciences*, **365**, 1801-1813.
- 426 Barraclough, T.G. & Humphreys, A.M. (2015) The evolutionary reality of species and higher
427 taxa in plants: a survey of post-modern opinion and evidence. *New Phytologist*, **207**,
428 291-296.
- 429 Barraclough, T.G. & Nee, S. (2001) Phylogenetics and speciation. *Trends in Ecology &*
430 *Evolution*, **16**, 391-399.
- 431 Blum, M.G.B., François, O. & Janson, S. (2006) The mean, variance and limiting distribution
432 of two statistics sensitive to phylogenetic tree balance. *The Annals of Applied*
433 *Probability*, **16**, 2195-2214.
- 434 Bortolussi, N., Durand, E., Blum, M. & François, O. (2012) apTreeshape: Analyses of
435 phylogenetic treeshape. R package version 1.4-5. [http://CRAN.R-](http://CRAN.R-project.org/package=apTreeshape)
436 [project.org/package=apTreeshape](http://CRAN.R-project.org/package=apTreeshape).
- 437 Burnham, K.P. & Anderson, D.R. (2002) *Model Selection and Multimodal Inference. A*
438 *practical Information-Theoretic Approach*, 2 edn. Springer-Verlag, New York.
- 439 Colless, D.H. (1982) Review of 'Phylogenetics: The Theory and Practice of Phylogenetic
440 Systematics', by E. O. Wiley. *Systematic Zoology*, **31**, 100-104.
- 441 Crisp, M.D. & Cook, L.G. (2009) Explosive radiation or cryptic mass extinction? Interpreting
442 signatures in molecular phylogenies. *Evolution*, **63**, 2257-2265.
- 443 Ericson, P.G.P., Anderson, C.L., Britton, T., Elzanowski, A., Johansson, U.S., Källersjö, M.,
444 Ohlson, J.I., Parsons, T.J., Zuccon, D. & Mayr, G. (2006) Diversification of Neaves:
445 integration of molecular sequence data and fossils. *Biology Letters*, **2**, 543-547.

- 446 Etienne, R.S. & Haegeman, B. (2012) A conceptual and statistical framework for adaptive
447 radiations with a key role for diversity dependence. *The American Naturalist*, **180**,
448 E75-E89.
- 449 Etienne, R.S., Haegeman, B., Stadler, T., Aze, T., Pearson, P.N., Purvis, A. & Phillimore,
450 A.B. (2012) Diversity-dependence bring molecular phylogenies closer to agreement
451 with the fossil record. *Proceedings of the Royal Society B-Biological Sciences*, **279**,
452 1300-1309.
- 453 Ezard, T., Fujisawa, T. & Barraclough, T.G. (2014) splits: SPecies' LImits by Threshold
454 Statistics. R package version 1.0-19/r51.
- 455 FitzJohn, R.G. (2012) Diversitree: comparative phylogenetic analyses of diversification in R.
456 *Methods in Ecology and Evolution*, **3**, 1084-1092.
- 457 FitzJohn, R.G., Maddison, W.P. & Otto, S.P. (2009) Estimating trait-dependent speciation
458 and extinction rates from incompletely resolved phylogenies. *Systematic Biology*, **58**,
459 595-611.
- 460 Fontaneto, D., Herniou, E.A., Boschetti, C., Caprioli, M., Melone, G., Ricci, C. &
461 Barraclough, T.G. (2007) Independently evolving species in asexual bdelloid rotifers.
462 *Plos Biology*, **5**, e87.
- 463 Fujisawa, T. & Barraclough, T.G. (2013) Delimiting species using single-locus data and the
464 generalized mixed Yule coalescent (GMYC) approach: A revised method and
465 evaluation on simulated datasets. *Systematic Biology*, **62**, 707-724.
- 466 Goldberg, E.E., Lancaster, L.T. & Ree, R.H. (2011) Phylogenetic inference of reciprocal
467 effects between geographic range evolution and diversification. *Systematic Biology*,
468 **60**, 451-465.
- 469 Harmon, L.J., Weir, J.T., Brock, C.D., Glor, R.E. & Challenger, W. (2008) GEIGER:
470 investigating evolutionary radiations. *Bioinformatics*, **24**, 129-131.
- 471 Hastie, T.J. & Tibshirani, R.J. (1990) *Generalized Additive Models*. Chapman and Hall.
- 472 Heard, S.B. (1992) Patterns in tree balance among cladistic, phenetic and randomly generated
473 phylogenetic trees. *Evolution*, **46**, 1818-1826.
- 474 Holt, B.G. & Jönsson, K.A. (2014) Reconciling hierarchical taxonomy with molecular
475 phylogenies. *Systematic Biology*, **63**, 1010-1017.
- 476 Hou, C., Humphreys, A.M., Thureborn, O. & Rydin, C. (2015) New insights into the
477 evolutionary history of *Gnetum* (Gnetales). *Taxon*, **64**, 239-253.
- 478 Hughes, C. & Eastwood, R. (2006) Island radiation on a continental scale: Exceptional rates
479 of plant diversification after uplift of the Andes. *Proceedings of the National Academy
480 of Sciences of the United States of America*, **103**, 10334-10339.

- 481 Humphreys, A.M. & Barraclough, T.G. (2014) The evolutionary reality of higher taxa in
 482 mammals. *Proceedings of the Royal Society B-Biological Sciences*, **281**, 1471-2954.
- 483 Jarvis, E.D., Mirarab, S., Aberer, A.J., Li, B., Houde, P., Li, C., Ho, S.Y.W., Faircloth, B.C.,
 484 Nabholz, B., Howard, J.T., Suh, A., Weber, C.C., da Fonseca, R.R., Li, J., Zhang, F.,
 485 Li, H., Zhou, L., Narula, N., Liu, L., Ganapathy, G., Boussau, B., Bayzid, M.S.,
 486 Zavidovych, V., Subramanian, S., Gabaldón, T., Capella-Gutiérrez, S., Huerta-Cepas,
 487 J., Rekepalli, B., Munch, K., Schierup, M., Lindow, B., Warren, W.C., Ray, D.,
 488 Green, R.E., Bruford, M.W., Zhan, X., Dixon, A., Li, S., Li, N., Huang, Y.,
 489 Derryberry, E.P., Bertelsen, M.F., Sheldon, F.H., Brumfield, R.T., Mello, C.V.,
 490 Lovell, P.V., Wirthlin, M., Schneider, M.P.C., Prosdocimi, F., Samaniego, J.A.,
 491 Velazquez, A.M.V., Alfaro-Núñez, A., Campos, P.F., Petersen, B., Sicheritz-Ponten,
 492 T., Pas, A., Bailey, T., Scofield, P., Bunce, M., Lambert, D.M., Zhou, Q., Perelman,
 493 P., Driskell, A.C., Shapiro, B., Xiong, Z., Zeng, Y., Liu, S., Li, Z., Liu, B., Wu, K.,
 494 Xiao, J., Yinqi, X., Zheng, Q., Zhang, Y., Yang, H., Wang, J., Smeds, L., Rheindt,
 495 F.E., Braun, M., Fjeldså, J., Orlando, L., Barker, F.K., Jönsson, K.A., Johnson, W.,
 496 Koepfli, K.-P., O'Brien, S., Haussler, D., Ryder, O.A., Rahbek, C., Willerslev, E.,
 497 Graves, G.R., Glenn, T.C., McCormack, J., Burt, D., Ellegren, H., Alström, P.,
 498 Edwards, S.V., Stamatakis, A., Mindell, D.P., Cracraft, J., Braun, E.L., Warnow, T.,
 499 Jun, W., Gilbert, M.T.P. & Zhang, G. (2014) Whole-genome analyses resolve early
 500 branches in the tree of life of modern birds. *Science*, **346**, 1320-1331.
- 501 Jetz, W., Thomas, G.H., Joy, J.B., Hartmann, K. & Mooers, A.O. (2012) The global diversity
 502 of birds in space and time. *Nature*, **491**, 444-448.
- 503 Leslie, A.B., Beaulieu, J.M., Rai, H.S., Crane, P.R., Donoghue, M.J. & Mathews, S. (2012)
 504 Hemisphere-scale differences in conifer evolutionary dynamics. *Proceedings of the*
 505 *National Academy of Sciences*, **109**, 16217-16221.
- 506 Maddison, W.P., Midford, P.E. & Otto, S.P. (2007) Estimating a binary character's effect on
 507 speciation and extinction. *Systematic Biology*, **56**, 701-710.
- 508 Moen, D. & Morlon, H. (2014) Why does diversification slow down? *Trends in Ecology &*
 509 *Evolution*, **29**, 190-197.
- 510 Monaghan, M.T., Wild, R., Elliot, M., Fujisawa, T., Balke, M., Inward, D.J., Lees, D.C.,
 511 Ranaivosolo, R., Eggleton, P., Barraclough, T.G. & Vogler, A.P. (2009) Accelerated
 512 species inventory on Madagascar using coalescent-based models of species
 513 delineation. *Systematic Biology*, **58**, 298-311.
- 514 Morlon, H., Parsons, T.L. & Plotkin, J.B. (2011) Reconciling molecular phylogenies with the
 515 fossil record. *Proceedings of the National Academy of Sciences*, **108**, 16327-16332.

516 Morlon, H., Potts, M.D. & Plotkin, J.B. (2010) Inferring the dynamics of diversification: A
517 coalescent approach. *Plos Biology*, **8**, e1000493.

518 Nagalingum, N.S., Marshall, C.R., Quental, T.B., Rai, H.S., Little, D.P. & Mathews, S.
519 (2011) Recent synchronous radiation of a living fossil. *Science*, **334**, 796-799.

520 Nee, S., Holmes, E.C., May, R.M. & Harvey, P.H. (1994) Extinction rates can be estimated
521 from molecular phylogenies. *Philosophical Transactions of the Royal Society of*
522 *London Series B-Biological Sciences*, **344**, 77-82.

523 Nee, S., May, R.M. & Harvey, P.H. (1994) The reconstructed evolutionary process.
524 *Philosophical Transactions of the Royal Society of London Series B-Biological*
525 *Sciences*, **344**, 305-311.

526 Papadopoulou, A., Bergsten, J., Fujisawa, T., Monaghan, M.T., Barraclough, T.G. & Vogler,
527 A.P. (2008) Speciation and DNA barcodes: testing the effects of dispersal on the
528 formation of discrete sequence clusters. *Philosophical Transactions of the Royal*
529 *Society B-Biological Sciences*, **363**, 2987-2996.

530 Paradis, E., Claude, J. & Strimmer, K. (2004) APE: Analyses of Phylogenetics and Evolution
531 in R language. *Bioinformatics*, **20**, 289-290.

532 Pons, J., Barraclough, T.G., Gomez-Zurita, J., Cardoso, A., Duran, D.P., Hazell, S., Kamoun,
533 S., Sumlin, W.D. & Vogler, A.P. (2006) Sequence-based species delimitation for the
534 DNA taxonomy of undescribed insects. *Systematic Biology*, **55**, 595-609.

535 R Development Core Team (2011) R: A language and environment for statistical computing.
536 R Foundation for Statistical Computing), Vienna, Austria.

537 Rabosky, D.L. (2006) Likelihood methods for detecting temporal shifts in diversification
538 rates. *Evolution*, **60**, 1152-1164.

539 Rabosky, D.L. (2009) Heritability of extinction rates links diversification patterns in
540 molecular phylogenies and fossils. *Systematic Biology*, **58**, 629-640.

541 Rabosky, D.L. (2014) Automatic detection of key innovations, rate shifts, and diversity-
542 dependence on phylogenetic trees. *Plos One*, **9**, e89543.

543 Reid, N.M. & Carstens, B.C. (2012) Phylogenetic estimation error can decrease the accuracy
544 of species delimitation: a Bayesian implementation of the general mixed Yule-
545 coalescent model. *Bmc Evolutionary Biology*, **12**, 196.

546 Rohlf, F.J., Chang, W.S., Sokal, R.R. & Kim, J. (1990) Accuracy of estimated phylogenies:
547 effects of tree topology and evolutionary model. *Evolution*, **44**, 1671-1684.

548 Rydin, C. & Korall, P. (2009) Evolutionary relationships in *Ephedra* (Gnetales), with
549 implications for seed plant phylogeny. *International Journal of Plant Sciences*, **170**,
550 1031-1043.

- 551 Shao, K. & Sokal, R.R. (1990) Tree balance. *Systematic Zoology*, **39**, 266-276.
- 552 Stadler, T. (2011) Simulating trees with a fixed number of extant species. *Systematic Biology*,
553 **60**, 676-684.
- 554 Stadler, T. (2012) TreeSim: Simulating trees under the birth-death model. [http://CRAN.R-](http://CRAN.R-project.org/package=TreeSim)
555 [project.org/package=TreeSim](http://CRAN.R-project.org/package=TreeSim).
- 556 Tang, C.Q., Humphreys, A.M., Fontaneto, D. & Barraclough, T.G. (2014) Effects of
557 phylogenetic reconstruction method on the robustness of species delimitation using
558 single-locus data. *Methods in Ecology and Evolution*, **5**, 1086-1094.
- 559 Valente, L.M., Savolainen, V. & Vargas, P. (2010) Unparalleled rates of species
560 diversification in Europe. *Proceedings of the Royal Society of London B: Biological*
561 *Sciences*, **22**, 1489-1496.
- 562 Wood, S.N. (2000) Modelling and smoothing parameter estimation with multiple quadratic
563 penalties. *Journal of the Royal Statistical Society (B)*, **62**, 413–428.
- 564 Wood, S.N. (2011) Fast stable restricted maximum likelihood and marginal likelihood
565 estimation of semiparametric generalized linear models. *Journal of the Royal*
566 *Statistical Society (B)*, **73**, 3–36.
- 567 Yule, G.U. (1925) A mathematical theory of evolution, based on the conclusions of Dr J C
568 Willis, F R S. *Philosophical Transactions of the Royal Society of London Series B-*
569 *Containing Papers of a Biological Character*, **213**, 21-87.
- 570

571 **Supporting Information**

572 The following supporting information is made available online as a single PDF file.

573

574 **SI Text**

575 **Text S1.** Selection and definition of bird clades

576 **Text S2.** Phylogenetic analyses for cycads and Gnetales

577 **Text S3.** Scaling GMYC rates to match those of the birth-death process

578 **Text S4.** R code used to calculate the non-cumulative stemminess index (St_N)

579

580 **SI Tables**

581 **Table S1.** Topological constraints and age priors for cycad and Gnetales Beast analyses

582 **Table S2.** Taxonomic diversity and sampling of empirical clades

583 **Table S3.** Parameter values for CRBD simulations based on empirical estimates

584 **Table S4.** Parameter values for VRBD simulations based on empirical estimates

585 **Table S5.** Models explaining the relationship between relative extinction rate (ϵ) and error
586 rates in CRBD trees simulated using general parameter values

587 **Table S6.** Fit of the MT-GMYC model to VRBD trees

588 **Table S7.** Tree characteristics of empirical and simulated trees of each size set

589

590 **SI Figures**

591 **Figure S1.** Lineages-through-time plots for trees simulated under CRBD models and the
592 MCC tree for each empirical clade

593 **Figure S2.** Taxonomic rank of hESUs for mammals, gymnosperms and birds

594 **Figure S3.** Lineages-through-time plots for trees simulated under CRBD models with
595 general parameter values

596 **Figure S4.** Lineages-through-time plots for trees simulated under VRBD models and the
597 MCC tree for each empirical clade

598

599 **SI References**

600 **Tables**

601

602 **Table 1.** Fit of null, single (ST) and multiple (MT) threshold GMYC models for empirical
 603 clades and inferences across the confidence set of models.

Clade	Lh (Null)	Lh (ST)	Lh (MT)	Models in 95% confidence set	hESUs	Mean threshold [Ma]
Carnivores	319.46	326.05***	328.17***	6 x MT, 8 x ST	20 (17–24)	14.1 (13.1–15.4)
Euungulates	475.90	487.52***	491.87***	7 x MT	24 (18–29)	12.7 (11.2–15.5)
Lagomorphs	42.89	48.76**	49.35**	3 x MT, 8 x ST	6 (2–11)	8.36 (5.53–13.5)
Conifers	738.5	756.5***	761.7***	9 x MT	83 (75–90)	16.4 (14.9–17.4)
Cycads	318.8	367.5***	369.4***	2 x MT, 1 x ST	14 (12–16)	6.83 (6.34–7.63)
Gnetales	11.2	15.1*	16.0**	4 x MT, 25 x ST	17 (7–31)	5.65 (2.70–19.1)
Afroaves	3230.72	3238.98***	3262.43***	6 x MT	76 (71–81)	14.4 (14.1–14.8)
Nightbirds	1181.56	1186.08**	1201.13***	5 x MT	64 (60–66)	11.1 (10.8–11.5)
Waterbirds	2445.82	2447.45	2448.83*	5 x MT, 41 x ST, Null	42 (1–1027)	33.3 (79–0.00)

604 Asterics denote significance compared to the null at P = 0.05 (*), P = 0.01 (**) and P ≤
 605 0.001 (***).

606 Lh = Log likelihood

607 Ma = million years

608

609 **Table 2.** Performance of the GMYC applied to CRBD trees simulated using empirical
610 parameter values for each study clade: the LR difference in fit between null and alternative
611 models for empirical (LR_{obs}) and simulated trees (LR_{sim}) and error rate (rejection of the null).

Clade	N	ST			MT		
		LR _{obs}	LR _{sim} (95%, 99%) ¹	Error rate	LR _{obs}	LR _{sim} (95%, 99%) ¹	Error rate
Carnivores	235	13.2	6.95, 10.3	6.64%	17.50	10.2, 13.0	21.1%
Euungulates	302	23.4	9.58, 13.0	9.50%	31.94	12.5, 18.4	31.1%
Lagomorphs	71	11.7	9.22, 14.9	12.1%	12.92	13.2, 19.4	31.9%
Conifers	489	36.0	17.9, 22.5	56.8%	46.4	24.2, 29.1	88.9%
Cycads	204	97.4	11.6, 17.6	30.8%	101.2	19.9, 26.1	68.3%
Gnetales	72	7.80	12.5, 16.5	33.0%	9.60	15.6, 10.7	63.4%
Afroaves	1132	16.5	9.51, 13.0	12.2%	63.4	12.4, 14.5	44.9%
Nightbirds	556	9.04	10.2, 12.4	16.1%	39.1	16.4, 21.3	54.6%
Waterbirds	1028	3.26	8.45, 10.4	10.7%	6.02	10.4, 13.6	36.5%

612 ¹95th and 99th percentiles

613 ST = single threshold GMYC method

614 MT = multiple threshold GMYC method

615 N = number of tips in phylogeny

616 LR = Likelihood ratio

Clade	$P \leq 0.05^1$	hESUs	Threshold [Mal]	Relative depth of shift	λ_{between}	λ_{within}	$\lambda_{\text{within}} / \lambda_{\text{between}}$	P_{between}	P_{within}
Carnivores	47.4%	13 (2-28.9)	18.3 (13.4-45.6)	0.39 (0.20-1.00)	0.065 (2.0e-05-0.38)	0.31 (0.059-0.55)	4.77	0.87 (0.00-12.7)	0.41 (0.23-0.64)
Euungulate s	100%	19 (11-34)	15.1 (12.0-21.9)	0.08 (0.047-0.16)	0.019 (0.0041-0.11)	0.33 (0.20-0.50)	17.37	0.86 (0.056-1.52)	0.43 (0.33-0.52)
Lagomorph s	74.5%	4 (2-12.4)	7.52 (4.92-11.3)	0.02 (0.33-0.0042)	5.6e-04 (6.1e-08-4.7e-02)	0.50 (0.25-1.54)	892.86	2.36 (-0.93-17.3)	0.45 (0.14-0.64)
Conifers	100%	29 (8.50-49.1)	28.0 (15.5-82.2)	0.031 (0.012-0.12)	0.0016 (0.00054-0.021)	0.071 (0.012-0.13)	44.38	1.34 (0.063-1.78)	0.84 (0.69-1.01)
Cycads	100%	28 (11-46)	6.79 (5.99-16.2)	0.00032 (0.00013-0.00099)	7.11e-05 (1.41e-05-9.81e-04)	0.32 (0.16-0.57)	4500.70	1.64 (0.94-2.35)	0.68 (0.41-0.88)
Gnetales	94%	6 (3-31.4)	6.59 (0.83-20.6)	0.0081 (0.0013-0.079)	7.35e-04 (4.48e-08-0.19)	0.24 (0.060-5.44)	326.53	1.76 (-0.31-12.9)	0.78 (0.048-1.16)
Affoaves	100%	49 (31-66)	31.4 (28.8-34.7)	0.60 (0.49-0.69)	0.088 (0.04-0.22)	0.85 (0.67-1.27)	9.66	0.98 (0.69-1.24)	2.22e-08 (1.03e-09-1.56e-07)
Nightbirds	100%	87 (63-112.1)	14.5 (11.7-15.5)	0.050 (0.031-0.076)	0.014 (0.0042-0.029)	0.32 (0.19-0.47)	22.86	1.00 (0.78-1.33)	0.41 (0.26-0.56)
Waterbirds	99%	15 (6.5-24)	40.2 (32.7-55.3)	0.20 (0.12-0.42)	0.015 (0.0050-0.092)	0.13 (0.096-0.19)	8.67	0.87 (0.0000082-1.56)	0.50 (0.45-0.55)

618 ¹Proportion of trees where single threshold (ST) GMYC detects a shift in diversification rate.

619 CI = confidence interval

620 VRBD = variable rate birth death

621 Ma = million years

622 **Table 4.** Performance of the GMYC applied to VRBD trees simulated using empirical
 623 parameter values for each study clade: the LR difference in fit between null and alternative
 624 models for empirical (LR_{obs}) and simulated trees (LR_{sim}).

Clade	ST		MT	
	LR_{obs}	LR_{sim} (95%, 99%) ¹	LR_{obs}	LR_{sim} (95%, 99%) ¹
Carnivores	13.2	15.5, 23.5	17.50	21.3, 29.7
Euungulates	23.4	84.6, 92.7	31.94	90.5, 100.2
Lagomorphs	11.7	80.0, 106.0	12.92	80.8, 106.3
Conifers	36.0	96.3, 107.6	46.4	100.9, 109.7
Cycads	97.4	332.1, 391.9	101.2	337.1, 395.7
Gnetales	7.80	62.9, 82.1	9.60	61.8, 83.9
Afroaves	16.5	319.3, 326.8	63.4	469.4, 498.6
Nightbirds	9.04	149.1, 153.3	39.1	156.2, 164.5
Waterbirds	3.26	85.4, 90.3	6.02	87.0, 93.8

625 ¹95th and 99th percentiles

626 ST = single threshold GMYC method

627 MT = multiple threshold GMYC method

628 LR = Likelihood ratio

629 **Figure legends**

630 **Figure 1.** Models of sharing and decoupling of speciation and extinction rates over time and
631 among clades. In clade independent models these parameters apply across the entire clade and
632 may be constant (CRBD) or variable (VRBD) over time. If variable over time, any rate shift
633 that occurs at a given time, T , will affect all lineages equally, irrespective of clade
634 membership. In contrast, in clade dependent models, speciation and extinction parameters will
635 vary over time as well as being decoupled among clades, due to occupation of different
636 geographical or ecological zones. Turnover through ongoing speciation and extinction will
637 operate independently among such clades, referred to as higher evolutionarily significant units
638 (hESUs). In this class of model, the threshold time, T , denotes the timing of the shift from
639 among to within clade processes. However, T does not denote the timing of any particular
640 event in the past, only the age of the most recent common ancestor of the oldest hESU, which
641 depends on the rate of turnover in that hESU. CRBD = constant-rate birth-death; VRBD =
642 variable-rate birth-death.

643

644 **Figure 2.** Error rates of the GMYC method applied above the species versus clade size (left)
645 and relative extinction rate (ϵ , right). Results for CRBD trees simulated using parameter
646 values estimated from the empirical clades (top row). Results for CRBD trees simulated using
647 general parameter values, with 100%, 75% and 50% of the species retained (rows 2–4).

648

649 **Figure 3.** Rule-of-thumb likelihood ratio (LR) values needed for significance against a CRBD
650 model based on relative extinction rate (ϵ) for the single-threshold (ST, top) and multiple-
651 threshold (MT, bottom) version of the GMYC, at $P = 0.05$ (dashed line, open circles) and $P =$
652 0.01 (solid line, filled circles; LR values from Table 2). Fitted linear models: $y=6.6x+7.4$ (ST,
653 $P = 0.05$); $y=8.1x+10.6$ (ST, $P = 0.01$); $y=8.0x+10.5$ (MT, $P = 0.05$); $y=9.5x+14.3$ (MT, $P =$
654 0.01). For example, a clade with average $\epsilon = 0.2$ would need a $LR \geq 16.2$ to reject the null in
655 favour of the MT-GMYC at $P = 0.01$ and a clade with average $\epsilon = 0.5$ would need a $LR \geq$
656 19.1 (blue lines).

Detecting evolutionarily significant units above the species level using the Generalized Mixed Yule Coalescent method

A.M. Humphreys, C. Rydin, K.A. Jønsson, D. Alsop, L.M. Callender-Crowe &
T.G. Barraclough

Supporting Information

Contents

SI Text

Text S1. Selection and definition of bird clades

Text S2. Phylogenetic analyses for cycads and Gnetales

Text S3. Scaling GMYC rates to match those of the birth-death process

Text S4. R code used to calculate the non-cumulative stemminess index (St_N)

SI Tables

Table S1. Topological constraints and age priors for cycad and Gnetales Beast analyses

Table S2. Taxonomic diversity and sampling of empirical clades

Table S3. Parameter values for CRBD simulations based on empirical estimates

Table S4. Parameter values for VRBD simulations based on empirical estimates

Table S5. Models explaining the relationship between relative extinction rate (ϵ) and error rates in CRBD trees simulated using general parameter values

Table S6. Fit of the MT-GMYC model to VRBD trees

Table S7. Tree characteristics of empirical and simulated trees of each size set

SI Figures

Figure S1. Lineages-through-time plots for trees simulated under CRBD models and the MCC tree for each empirical clade

Figure S2. Taxonomic rank of hESUs for mammals, gymnosperms and birds

Figure S3. Lineages-through-time plots for trees simulated under CRBD models with general parameter values

Figure S4. Lineages-through-time plots for trees simulated under VRBD models and the MCC tree for each empirical clade

SI References

SI Text

SI Text S1. SELECTION AND DEFINITION OF BIRD CLADES

Bird clades selected for analysis were generated by pruning the Hackett-backbone maximum clade credibility (MCC) tree of Jetz *et al.* (2012) to contain only the desired species. In addition, 500 posterior trees were obtained for each species set from birdtree.org (Jetz *et al.* 2012). The first clade is equivalent to Jarvis *et al.*'s (2014) Afroaves and includes groups such as the New World vultures, eagles, owls, mousebirds, cuckoo-roller, trogons, hornbills, woodpeckers, kingfishers, toucans, jacamars and bee-eaters. The second clade is Hackett *et al.*'s (2008) Caprimulgiformes (nightjars) and Apodiformes (hummingbirds and swifts) and Jarvis *et al.*'s (2014) Caprimulgimorphae, plus the kagu (*Rhynochetos*) and sunbittern (*Eurypyga*). Ericson *et al.* (2006) refer to this group as “nightbirds (except owls), swifts and hummingbirds”. We adopt this name here (“nightbirds” for short), whilst being aware that as a whole, the clade is unsupported. The third clade is Jarvis *et al.*'s (2014) “core waterbirds” (including loons, penguins, fulmars, cormorants, ibises, herons and pelicans) plus turacos, rails, bustards, cuckoos, pigeons, mesites, sandgrouses, flamingos, grebes and the hoatzin. This forms a clade in the Hackett backbone tree of Jetz *et al.* (2012) although a relationship between core waterbirds and cuckoos and pigeons has not been found in other studies. We refer to this clade as “waterbirds”.

SI Text S2. PHYLOGENETIC ANALYSES FOR CYCADS AND GNETALES

Phylogenies for cycads and Gnetales were generated using published sequences for chloroplast regions matK and rbcL, 18S of nuclear ribosomal DNA and, for cycads, the nuclear phytochrome-P gene (PHYP; Rydin & Korall 2009; Nagalingum *et al.* 2011; Hou *et al.* 2015). Sequences were aligned manually in Mesquite 2.74 (Maddison & Maddison 2010) because there were no alignment ambiguities. Using *Ginkgo biloba* as an outgroup, a RAxML (Stamatakis 2006; Stamatakis, Hoover & Rougemont 2008) tree was first inferred for each dataset. Then identical sequences were removed to improve convergence of downstream analyses. Based on the trimmed dataset, time-calibrated trees were generated in Beast (Drummond & Rambaut 2007; Drummond *et al.* 2012) using a number of topological constraints and age priors (Table S1), a GTR + G substitution model, unlinked among gene regions, a birth-death tree prior (Gernhard 2008) and either the RAxML (cycads) or a random (Gnetales) starting tree. A random starting tree together with more topological constraints improved convergence and sampling of parameters for Gnetales. For each dataset, four runs of 80×10^6 generations, sampling every 1000, were performed. Convergence of runs and

sampling and mixing of parameters were assessed in Tracer (Rambaut & Drummond 2007), measured as a combined effective sample size of ~ 200 . A set of 20,000 trees was sampled from across all four (cycads) or three (Gnetales) runs post burnin and tree statistics were summarised on the MCC tree from that set, retaining the node heights of the MCC tree. Analyses were run on the Cipres Science Gateway (Miller *et al.* 2012).

SI Text S3. SCALING GMYC RATES TO MATCH THOSE OF THE BIRTH-DEATH PROCESS

Diversification rates inferred from the best-fitting MT-GMYC models are on average much higher than those inferred from CRBD models (except for waterbirds; Table S4). This is because the equations underlying the GMYC are quite different from those underlying the CRBD process. Preliminary analyses showed that simulating trees using the raw GMYC estimates produced trees that were extremely young, with an extremely deep relative shift position (i.e. the shift is pushed back in an attempt to accommodate the predefined absolute shift time but the process is so quick that the tree grows to the specified number of tips before it reaches the specified shift time). Therefore the GMYC rates were scaled to match those expected under a CRBD process by dividing the average GMYC rate with the CRBD diversification rate. This amendment allowed fixing the position of the shift in absolute time at a position that matched the empirically inferred threshold time.

SI Text S4. R CODE USED TO CALCULATE THE NON-CUMULATIVE STEMMINESS INDEX (St_N)

```
# Function for calculating Rohlf's Stemminess Index on a
  single tree
# Reference: Rohlf, F.J., Chang, W.S., Sokal, R.R. & Kim, J.
  (1990) Accuracy of estimated phylogenies: effects of tree
  topology and evolutionary model. Evolution, 44, 1671-1684.

stemminess= function(tr){t <- Ntip(tr)
h <- numeric()
for (i in (1:length(tr$edge[,1]))) {
  times <- branching.times(tr)
  names(times) <- c((Ntip(tr)+1):(Ntip(tr)+Nnode(tr)))
  if (tr$edge[i, 2]>=(Ntip(tr)+1))
  h[i] <- times[names(times)==tr$edge[i,1]]
  else h[i] <- 0
}
h <- h[which(h>0)]
w <- tr$edge.length[which(h>0)]
ST <- sum(w/h)
St <- (1/(t-2))*ST
return(St)
}
```

SI Tables

SI Table S1. Topological constraints and age priors used in the Beast analyses for cycads and Gnetales.

Taxon ¹	Age prior [Ma]	Reference
Cycadales		
Cycadales	208.0 ± 2	(Nagalingum <i>et al.</i> 2011)
Cycadales excl. <i>Cycas</i>	120.6 ± 2	(Nagalingum <i>et al.</i> 2011)
<i>Cycas</i>	10.5 ± 1	(Nagalingum <i>et al.</i> 2011)
<i>Encephalartos</i>	9.5 ± 0.5	(Nagalingum <i>et al.</i> 2011)
<i>Zamia</i>	8.0 ± 1	(Nagalingum <i>et al.</i> 2011)
<i>Macrozamia</i>	5.0 ± 1	(Nagalingum <i>et al.</i> 2011)
<i>Ceratozamia</i>	7.5 ± 1.5	(Nagalingum <i>et al.</i> 2011)
<i>Encephalartos</i> + <i>Lepidozamia</i>	40.0 ± 2	(Nagalingum <i>et al.</i> 2011)
<i>Bowenia</i> + its sister clade	102.0 ± 2	(Nagalingum <i>et al.</i> 2011)
Root height (gymnosperms)	387.0 ± 0.005	(Magallón 2010) ²
Gnetales		
Gnetales	167 ± 2	(Rydin <i>et al.</i> 2006; Ickert-Bond, Rydin & Renner 2009)
<i>Welwitschia</i> + <i>Gnetum</i>	111.4 ± 2	(Ickert-Bond, Rydin & Renner 2009)
<i>Gnetum</i>	None	(Won & Renner 2006; Hou <i>et al.</i> 2015)
<i>Gnetum</i> _South America	None	(Won & Renner 2006; Hou <i>et al.</i> 2015)
<i>Gnetum</i> _trees	None	(Won & Renner 2006; Hou <i>et al.</i> 2015)
<i>Gnetum</i> _Asia I	None	(Won & Renner 2006; Hou <i>et al.</i> 2015)
<i>Gnetum</i> _Asia II	None	(Won & Renner 2006; Hou <i>et al.</i> 2015)
<i>Ephedra</i>	30.39 ± 5	(Ickert-Bond, Rydin & Renner 2009)
<i>Ephedra</i> _New World	None	(Rydin & Korall 2009)
<i>Ephedra</i> _China	None	(Rydin & Korall 2009)
<i>Ephedra</i> _Asia I+Horn of Africa	None	(Rydin & Korall 2009)
<i>Ephedra</i> _Asia I	None	(Rydin & Korall 2009)
<i>Ephedra</i> _Asia I+II+Horn of Africa	None	(Rydin & Korall 2009)
<i>Ephedra</i> _Asia II	None	(Rydin & Korall 2009)
Root height (gymnosperms)	387.0 ± 0.005	(Magallón 2010) ²

¹All listed clades were constrained to be monophyletic. Some were also given an age prior.

²The oldest estimate for seed plants (node 9; Magallón 2010). If gymnosperms are monophyletic (node 10), it is equivalent to their stem age.

Ma = million years

SI Table S2. Taxonomic diversity¹ and sampling of empirical clades.

Clade	Orders	Families	Genera	Species	Sampling
Carnivores	1	16	123	285	83%
Euungulates	2	24	138	346	87%
Lagomorphs	1	2	12	92	77%
Conifers	1	6	72	~550 ²	~89%
Cycads	1	2	10	~300 ²	~68%
Gnetales	1	3	3	~80	~90%
Afroaves	7	21	218	1132	100% ³
Nightbirds	3	10	148	566	100% ³
Waterbirds	17	31	223	1028	100% ³

¹Numbers were taken from Wilson & Reeder (2005) and IUCN (2011) species lists for mammals; Jetz *et al.* (2012) for birds, where the taxonomy is mainly based on BirdLife International (www.birdlife.org) and the International Ornithologists' Committee (www.worldbirdnames.org); Leslie *et al.* (2012) and Eckenwalder (2009) for conifers; Nagalingum *et al.* (2011) and the World List of Cycads (www.cycadlist.org) for cycads; and Kubitzki (1990) for Gnetales.

²These figures are low compared to some recent estimates. It is uncertain how much of recent increases in species numbers is due to true species discovery and how much to do with taxonomic splitting (e.g. Eckenwalder 2009).

³DNA data exist for two thirds of the species on average. The remainder have been modelled in by the authors based on prior taxonomic knowledge (Jetz *et al.* 2012).

SI Table S3. Parameter values for CRBD simulations based on estimates across each of the nine empirical clades.

Clade	N	μ	λ	μ/λ
Carnivores	235	0.00 (0.00–0.00)	0.12 (0.11–0.12)	0.00 (0.00–0.00)
Euungulates	302	0.032 (0.01–0.05)	0.13 (0.11–0.14)	0.25 (0.08–0.35)
Lagomorphs	71	0.030 (0.00–0.10)	0.19 (0.16–0.23)	0.16 (0.00–0.44)
Conifers	489	0.30	0.31	0.98
Cycads	204	0.30 (0.25–0.36)	0.31 (0.26–0.36)	0.98 (0.96–0.99)
Gnetales	72	0.38 (0.23–0.71)	0.38 (0.23–0.71)	1.00 (1.00–1.00)
Afroaves	1132	0.038 (0.012–0.075)	0.12 (0.097–0.15)	0.32 (0.13–0.51)
Nightbirds	566	0.067 (0.041–0.091)	0.13 (0.11–0.16)	0.50 (0.35–0.59)
Waterbirds	1028	0.018 (0.0037–0.033)	0.083 (0.071–0.097)	0.22 (0.050–0.35)

Estimates are based on 500 trees apart from for conifers where 1 empirical tree was used only.

Estimates for mammals are from Humphreys & Barraclough (2014) and are provided here for comparison only.

N = number of tips

SI Table S4. Parameter values for VRBD simulations based on estimates from the best-fitting GMYC models for each of the nine empirical clades.

Clade	N	λ_2	λ_1	λ_1/λ_2	p_2	p_1	<i>T</i>	Scale
Carnivores	235	0.19	0.42	2.21	0.40	0.25	13.1–15.4	2.58
Euungulates	302	0.062	0.82	13.23	0.79	0.17	11.2–15.5	4.54
Lagomorphs	71	0.0092	1.60	173.91	2.65	0.00	5.53–13.5	5.05
Conifers	489	0.016	0.15	9.38	0.93	0.49	14.9–17.4	8.3
Cycads	204	0.011	2.45	222.73	1.14	0.076	6.34–7.63	123.1
Gnetales	72	0.0082	0.41	50.16	1.47	0.34	2.70–19.1	20.9
Afroaves	1132	12.1	0.44	0.04	-1.63	0.25	14.1–14.8	76.8
Nightbirds	566	0.16	1.34	8.38	0.54	3.6×10^{-8}	10.8–11.5	11.5
Waterbirds	1028	0.0097	0.075	7.73	3.27	0.51	33.3	0.65

N = number of tips

λ_1 = pre-shift / within-hESU rate

λ_2 = post-shift / among-hESU rate

p_1 = pre-shift / within-hESU scaling parameter

p_2 = post-shift / among-hESU scaling parameter

T = shift position (for waterbirds mean threshold time is used; for all others the range estimated from confidence set of models is used)

Scale = average GMYC rate divided by the CRBD diversification rate ($\lambda-\mu$)

SI Table S5. Models for explaining the relationship between relative extinction rate (ϵ) and error rates in CRBD trees simulated using general parameters values.

Dataset	Model	F	D.f.	GCV	P	R²
ST 100%	Gaussian	19.13	15.35	140.47	< 0.001	0.75
MT 100%	Linear	105.4	16.00	-	<< 0.001	0.86
ST 75%	Gaussian	14.83	14.98	97.01	< 0.001	0.73
MT 75%	Gaussian	40.44	15.24	79.94	<< 0.001	0.87
ST 50%	Gaussian	7.32	14.77	59.21	0.0026	0.56
MT 50%	Gaussian	13.74	14.86	105.18	< 0.001	0.72

SI Table S6. Fit of the MT-GMYC model to trees simulated with the VRBD model.

Clade	Lh (Null)¹	Lh (ST)¹	Lh (MT)¹	MT > ST²
Carnivores	375.7	379.0	381.6	46 (60)
Euungulates	573.1	600.5	602.2	19 (42)
Lagomorphs	67.7	83.7	84.8	14 (30)
Conifers	1394.0	1425.0	1427.0	23 (63)
Cycads	211.3	328.7	329.8	6 (27)
Gnetales	97.7	112.9	130.8	10 (24)
Afroaves	2666.0	2797.0	2837.0	67 (69)
Nightbirds	1197.0	1251.0	1256.0	51 (51)
Waterbirds	2930.0	2955.0	2956.0	11 (37)

¹Average across 100 trees

²Number of trees where the MT-GMYC fits the data better than ST-GMYC at $\Delta\text{AIC} \geq 5$ (in brackets, at $\Delta\text{AIC} \geq 3$).

SI Table S7. Tree characteristics of empirical and simulated trees of each size set.

Dataset	I_c			I_s			$S_{N_c}^*$		
	MCC	CRBD ¹	VRBD ¹	MCC	CRBD ¹	VRBD ¹	MCC	CRBD ¹	VRBD ¹
Carnivores	0.81	0.16 (-1.15–2.35)	-0.0011 (-1.37–1.94)	0.75	0.15 (-0.82–1.88)	-0.040 (-0.97–1.63)	0.70	0.67 (0.51–0.94)	0.74 (0.54–1.25)
Euungulates	4.88	0.059 (-1.17–2.28)	-0.10 (-1.37–1.58)	4.15	0.056 (-0.89–1.96)	-0.032 (-1.03–1.33)	0.57	0.70 (0.55–1.04)	1.14 (0.75–2.04)
Lagomorphs	1.16	0.022 (-1.13–1.81)	-0.11 (-1.33–1.60)	0.90	0.024 (-0.79–1.52)	-0.10 (-0.91–1.37)	1.08	0.65 (0.47–1.43)	0.93 (0.44–23.4)
Conifers	2.76	-0.060 (-1.15–1.71)	-0.071 (-1.13–1.67)	2.44	-0.057 (-0.88–1.37)	-0.087 (-0.85–1.37)	1.39	1.69 (1.19–3.80)	5.45 (1.88–16.2)
Cycads	1.59	-0.026 (-1.23–2.11)	-0.11 (-1.22–1.28)	1.37	-0.0064 (-0.89–1.83)	-0.068 (-0.90–1.14)	1.75	1.43 (0.86–3.36)	123.4 (35.5–446.5)
Gnetales	0.16	-0.091 (-1.13–1.76)	-0.19 (-1.11–1.63)	0.13	-0.097 (-0.85–1.55)	-0.13 (-0.80–1.27)	0.52	1.33 (0.58–3.93)	8.27 (0.63–143.3)
Afroaves	4.04	-0.10 (-1.31–1.65)	-0.022 (-0.96–1.53)	3.28	-0.10 (-0.93–1.25)	-0.032 (-0.74–1.19)	0.63	0.76 (0.64–1.01)	0.45 (0.44–0.48)
Nightbirds	6.17	-0.092 (-1.23–1.85)	0.028 (-1.30–1.51)	5.54	-0.10 (0.91–1.46)	0.0041 (-0.89–1.28)	0.51	0.79 (0.64–1.09)	1.84 (1.24–3.36)
Waterbirds	2.45	-0.050 (-1.32–1.68)	-0.10 (-1.27–1.64)	2.29	-0.088 (-0.99–1.42)	-0.10 (-0.97–1.31)	0.53	0.72 (0.61–0.94)	0.78 (0.64–1.07)

¹For simulated trees median and 95% confidence interval are shown.

I_c = Colless' index of tree imbalance

I_s = Sackin's index of tree imbalance

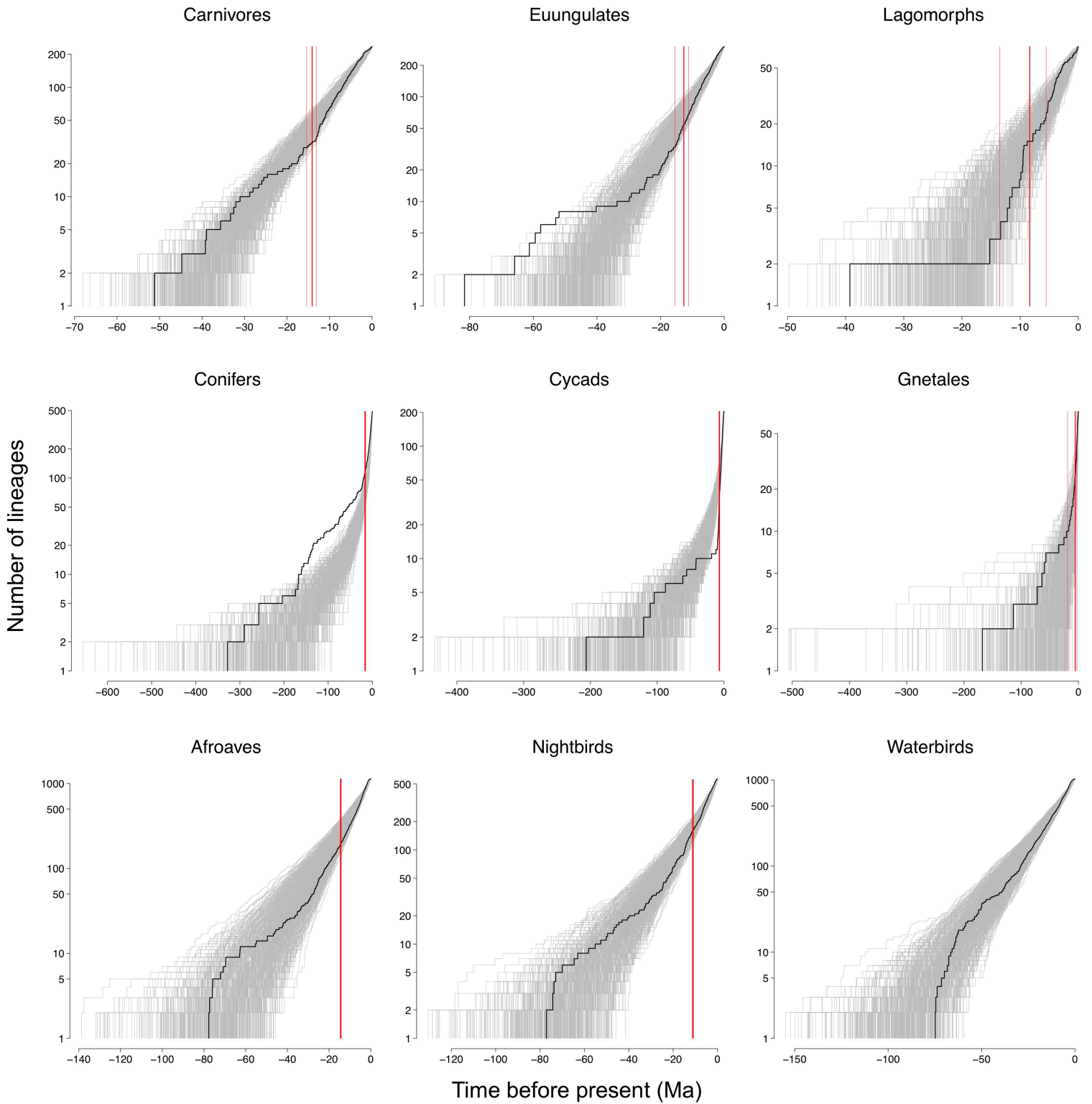
$S_{N_c}^*$ = Rohlf's non-cumulative stemminess index

MCC = maximum clade credibility tree

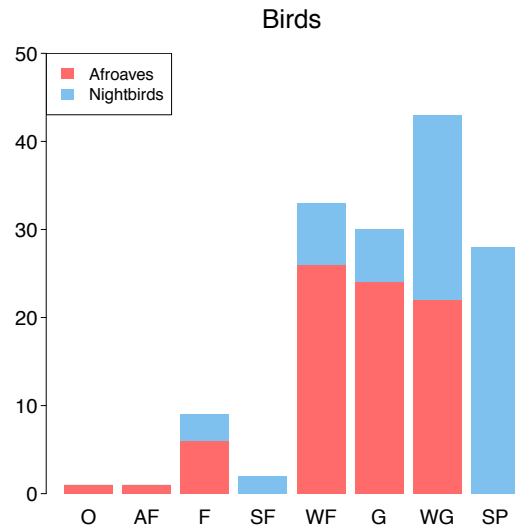
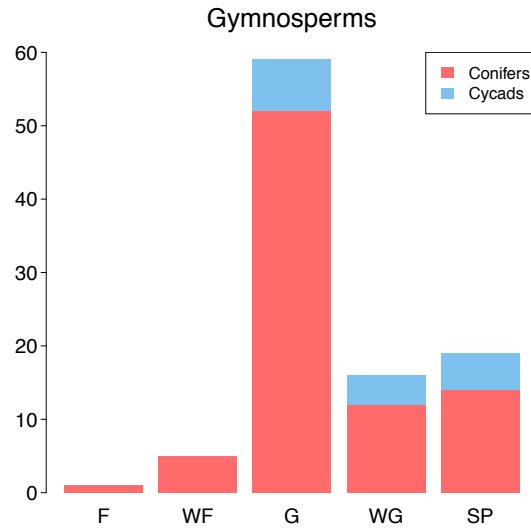
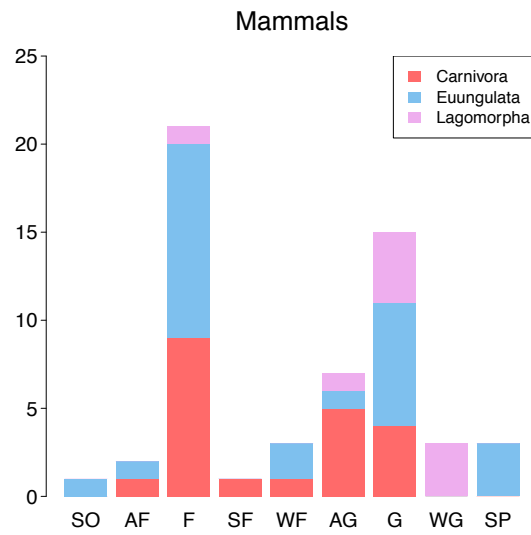
CRBD = trees simulated under a constant rate birth-death process

VRBD = trees simulated under a variable rates birth-death process

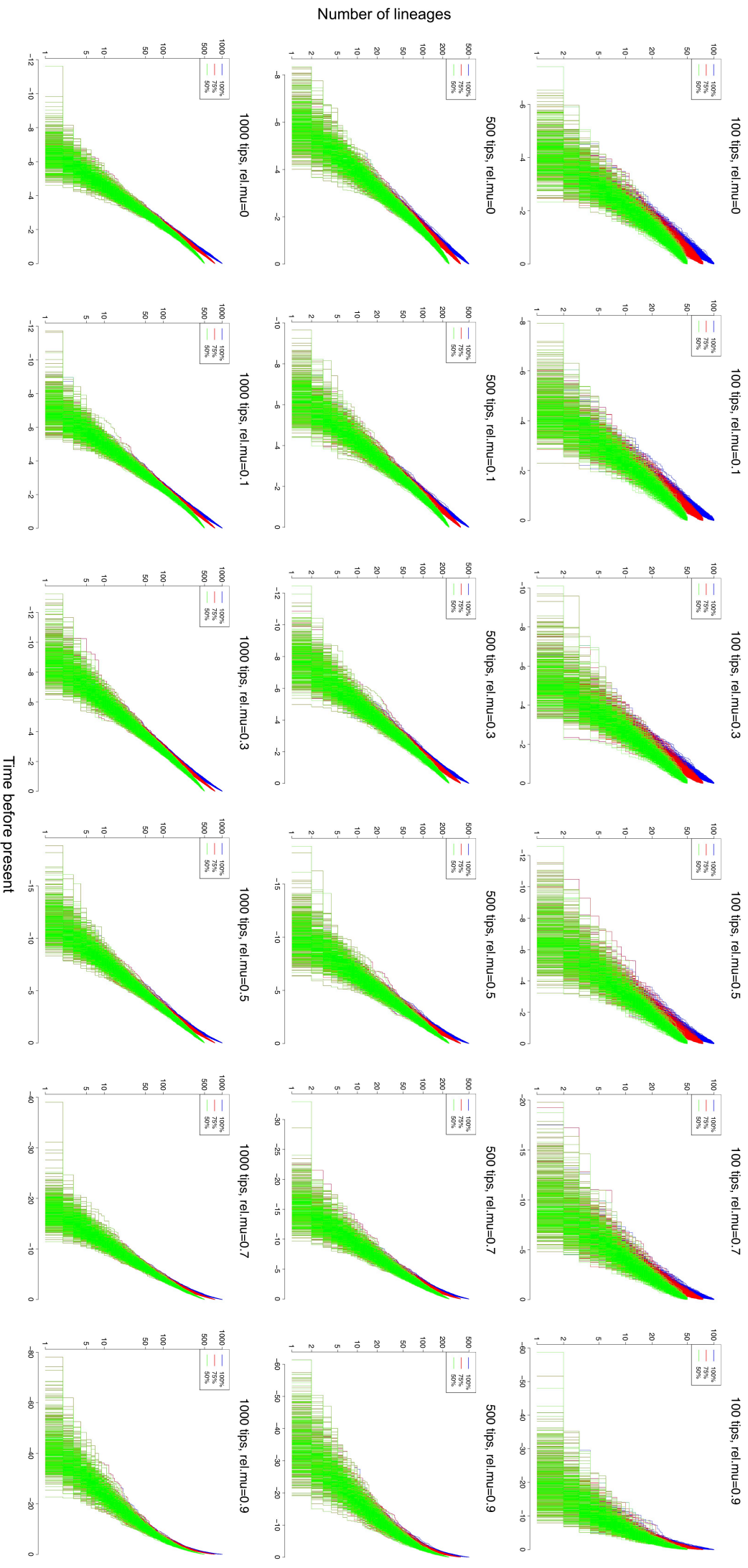
SI Figures



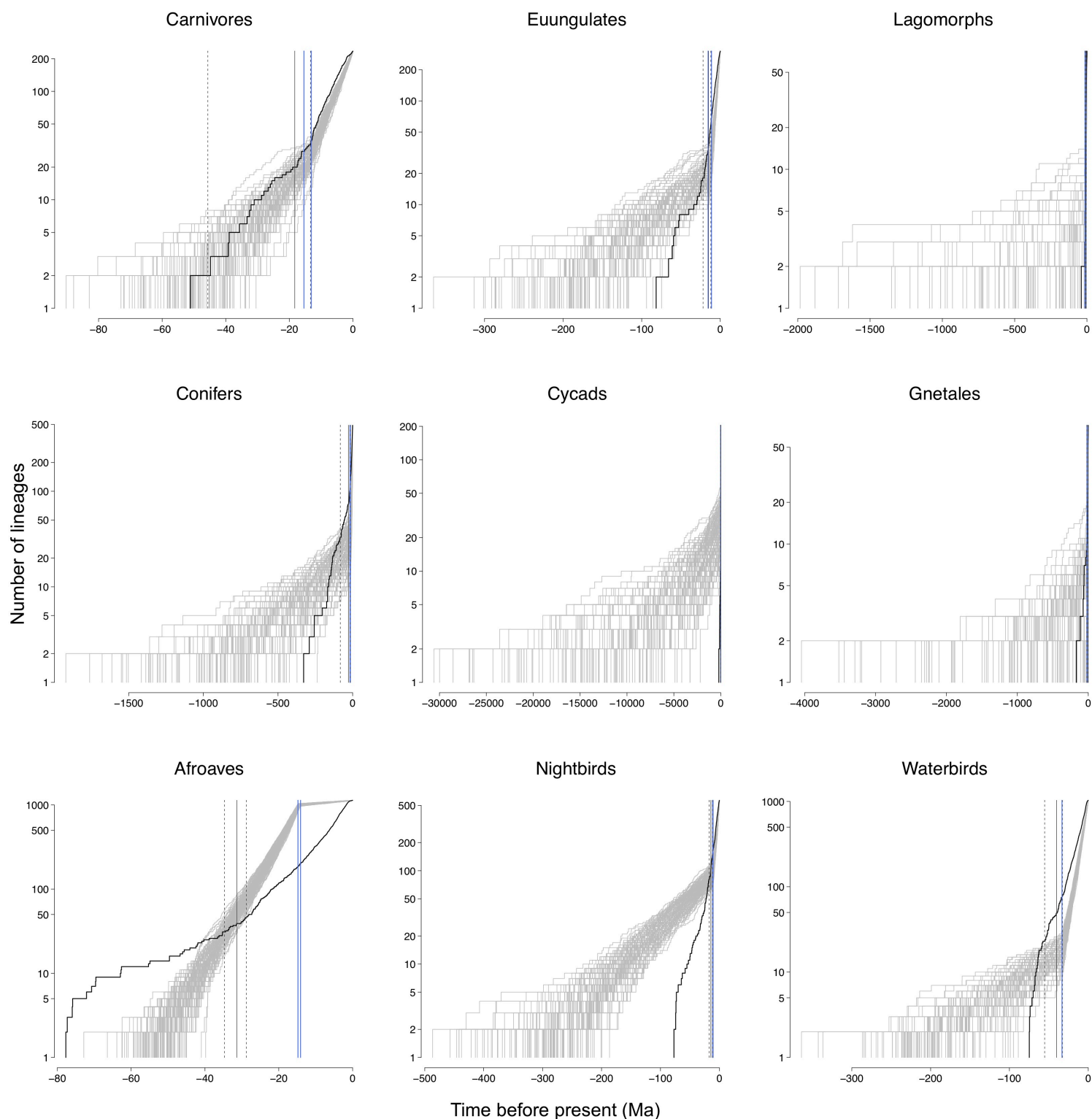
SI figure S1. Lineages-through-time plots for trees simulated under CRBD models (grey) and the MCC tree for each empirical clade (black), with the threshold range (red, vertical lines) inferred from the 95% confidence set of best GMYC models.



SI figure S2. Taxonomic rank of hESUs inferred for the a) mammal, b) gymnosperm and c) bird clades, where empirical results differ significantly from those expected under the constant-rate birth-death model (i.e. excluding results for Gnetales and waterbirds). hESUs = higher evolutionarily significant units. O = Order, SO = “Suborder” (comprises one suborder, one infraorder and one superfamily), AF = Above-family, F = Family, SF = Subfamily, WF = Within-family, AG = Above-genus, G = genus, WG = Within-genus, SP = Species. (Bold text denotes formal taxonomic ranks.)



SI figure S3. Lineages-through-time plots for trees simulated under constant-rate birth-death models with general parameter values and 100% (blue), 75% (red) and 50% (green) sampling. Note that the plots are identical early on, with differences appearing only toward the present due to removal of tips.



SI figure S4. Lineages-through-time plots for trees simulated under VRBD models (grey) and the MCC tree for each empirical clade (black). Vertical lines are threshold times inferred with the GMYC method for simulated (grey) and empirical (blue) trees. The empirical threshold time overlaps with range of threshold times under which trees were simulated for all clades except those simulated using Afroaves parameter values. For trees simulated using lagomorph and Gnetales parameter values the overlap was almost perfect, for euungulate and cycad-based trees inferred shift times extended a little deeper and for the other five clades the range of inferred shift times extended much deeper than the range under which they were simulated.

SI References

- Drummond, A. & Rambaut, A. (2007) BEAST: Bayesian evolutionary analysis by sampling trees. *BMC Evolutionary Biology*, **7**, 214.
- Drummond, A.J., Suchard, M.A., Xie, D. & Rambaut, A. (2012) Bayesian phylogenetics with BEAUti and the BEAST 1.7. *Molecular Biology and Evolution*, **29**, 1969-1973.
- Eckenwalder, J.E. (2009) *Conifers of the World*. Timber Press, Inc., Portland, Oregon.
- Ericson, P.G.P., Anderson, C.L., Britton, T., Elzanowski, A., Johansson, U.S., Källersjö, M., Ohlson, J.I., Parsons, T.J., Zuccon, D. & Mayr, G. (2006) Diversification of Neoaves: integration of molecular sequence data and fossils. *Biology Letters*, **2**, 543-547.
- Gernhard, T. (2008) The conditioned reconstructed process. *Journal of Theoretical Biology*, **253**, 769-778.
- Hackett, S.J., Kimball, R.T., Reddy, S., Bowie, R.C.K., Braun, E.L., Braun, M.J., Chojnowski, J.L., Cox, W.A., Han, K.-L., Harshman, J., Huddleston, C.J., Marks, B.D., Miglia, K.J., Moore, W.S., Sheldon, F.H., Steadman, D.W., Witt, C.C. & Yuri, T. (2008) A phylogenomic study of birds reveals their evolutionary history. *Science*, **320**, 1763-1768.
- Hou, C., Humphreys, A.M., Thureborn, O. & Rydin, C. (2015) New insights into the evolutionary history of *Gnetum* (Gnetales). *Taxon*, **64**, 239-253.
- Humphreys, A.M. & Barraclough, T.G. (2014) The evolutionary reality of higher taxa in mammals. *Proceedings of the Royal Society B-Biological Sciences*, **281**, 1471-2954.
- Ickert-Bond, S.M., Rydin, C. & Renner, S.S. (2009) A fossil-calibrated relaxed clock for *Ephedra* indicates an Oligocene age for the divergence of Asian and New World clades and Miocene dispersal into South America. *Journal of Systematics and Evolution*, **47**, 444-456.
- IUCN (2011) The IUCN Red List of Threatened Species, Version 3.1 (2011.2) [Accessed October, 2011].
- Jarvis, E.D., Mirarab, S., Aberer, A.J., Li, B., Houde, P., Li, C., Ho, S.Y.W., Faircloth, B.C., Nabholz, B., Howard, J.T., Suh, A., Weber, C.C., da Fonseca, R.R., Li, J., Zhang, F., Li, H., Zhou, L., Narula, N., Liu, L., Ganapathy, G., Boussau, B., Bayzid, M.S., Zavidovych, V., Subramanian, S., Gabaldón, T., Capella-Gutiérrez, S., Huerta-Cepas, J., Rekepalli, B., Munch, K., Schierup, M., Lindow, B., Warren, W.C., Ray, D., Green, R.E., Bruford, M.W., Zhan, X., Dixon, A., Li, S., Li, N., Huang, Y., Derryberry, E.P., Bertelsen, M.F., Sheldon, F.H., Brumfield, R.T., Mello, C.V., Lovell, P.V., Wirthlin, M., Schneider, M.P.C., Prosdocimi, F., Samaniego, J.A.,

- Velazquez, A.M.V., Alfaro-Núñez, A., Campos, P.F., Petersen, B., Sicheritz-Ponten, T., Pas, A., Bailey, T., Scofield, P., Bunce, M., Lambert, D.M., Zhou, Q., Perelman, P., Driskell, A.C., Shapiro, B., Xiong, Z., Zeng, Y., Liu, S., Li, Z., Liu, B., Wu, K., Xiao, J., Yinqi, X., Zheng, Q., Zhang, Y., Yang, H., Wang, J., Smeds, L., Rheindt, F.E., Braun, M., Fjeldså, J., Orlando, L., Barker, F.K., Jönsson, K.A., Johnson, W., Koepfli, K.-P., O'Brien, S., Haussler, D., Ryder, O.A., Rahbek, C., Willerslev, E., Graves, G.R., Glenn, T.C., McCormack, J., Burt, D., Ellegren, H., Alström, P., Edwards, S.V., Stamatakis, A., Mindell, D.P., Cracraft, J., Braun, E.L., Warnow, T., Jun, W., Gilbert, M.T.P. & Zhang, G. (2014) Whole-genome analyses resolve early branches in the tree of life of modern birds. *Science*, **346**, 1320-1331.
- Jetz, W., Thomas, G.H., Joy, J.B., Hartmann, K. & Mooers, A.O. (2012) The global diversity of birds in space and time. *Nature*, **491**, 444-448.
- Kubitzki, K. (1990) Gnetaceae. *The families and genera of vascular plants, vol. 1, Pteridophytes and gymnosperms* (eds K.U. Kramer & P.S. Green), pp. 383-386. Springer, Berlin, Heidelberg.
- Leslie, A.B., Beaulieu, J.M., Rai, H.S., Crane, P.R., Donoghue, M.J. & Mathews, S. (2012) Hemisphere-scale differences in conifer evolutionary dynamics. *Proceedings of the National Academy of Sciences*, **109**, 16217-16221.
- Maddison, W.P. & Maddison, D.R. (2010) Mesquite: A modular system for evolutionary analysis. Version 2.74. <http://mesquiteproject.org>.
- Magallón, S. (2010) Using fossils to break long branches in molecular dating: A comparison of relaxed clocks applied to the origin of angiosperms. *Systematic Biology*, **59**, 384-399.
- Miller, M., Holder, M., Vos, R., Midford, P., Liebowitz, T., Chan, L., Hoover, P. & Warnow, T. (2012) The CIPRES Portals. CIPRES. http://www.phylo.org/sub_sections/portal.
- Nagalingum, N.S., Marshall, C.R., Quental, T.B., Rai, H.S., Little, D.P. & Mathews, S. (2011) Recent synchronous radiation of a living fossil. *Science*, **334**, 796-799.
- Rambaut, A. & Drummond, A.J. (2007) Tracer v1.4. Available from <http://beast.bio.ed.ac.uk/Tracer>.
- Rydin, C. & Korall, P. (2009) Evolutionary relationships in *Ephedra* (Gnetales), with implications for seed plant phylogeny. *International Journal of Plant Sciences*, **170**, 1031-1043.
- Rydin, C., Pedersen, K.R., Crane, P.R. & Friis, E.M. (2006) Former diversity of *Ephedra* (Gnetales): Evidence from Early Cretaceous seeds from Portugal and North America. *Annals of Botany*, **98**, 123-140.

- Stamatakis, A. (2006) RAxML-VI-HPC: Maximum likelihood-based phylogenetic analyses with thousands of taxa and mixed models. *Bioinformatics*, **22**, 2688-2690.
- Stamatakis, A., Hoover, P. & Rougemont, J. (2008) A rapid bootstrap algorithm for the RAxML web servers. *Systematic Biology*, **57**, 758-771.
- Wilson, D.E. & Reeder, D.A. (2005) *Mammal Species of the World: A Taxonomic and Geographic Reference*, 3 edn. Johns Hopkins Univ. Press, Baltimore.
- Won, H. & Renner, S.S. (2006) Dating dispersal and radiation in the gymnosperm *Gnetum* (Gnetales) - Clock calibration when outgroup relationships are uncertain. *Systematic Biology*, **55**, 610-622.